

Cosmic Super String Detection Using Dilated
Convolutional Neural Network with focal loss

Mohammed Hasin Ishrak
School of Engineering , BRAC University

Abstract

Cosmic string are objects of great importance and investigation for cosmic string has been done from last 20 years. There are a lot of models to detect cosmic string. But a very few are to detect the location of cosmic string. We propose a framework to detect the location of cosmic string. We used dilated convolutional net with focal loss instead of cross-entropy to improved the performance of the framework on weak samples. The neural network we trained is able to detect and locate cosmic string on noiseless CMB temperature map down to a string tension of less than $G_{\mu}=5 \times 10^{-9}$. We expect to use more accurate simulation to produce data set to improve the confidence of the model.

Key words

Cosmic background radiation-physics simulation-cosmology-cosmic string-machine learning -cosmic data science-large scale structure of universe-early universe

Contents

0.1	Introduction	3
0.1.1	Cosmic Microwave background	3
0.1.2	Cosmic String	4
0.1.3	Cosmic Super String	7
0.1.4	Cosmic string in String theory and QFT	8
0.1.5	Observation of Cosmic String	9
0.2	Non-machine learning Approaches	13
0.3	Machine Learning Approach	15
0.4	Neural Network prediction for String Location	17
0.4.1	Supervised Learning	17
0.4.2	Neural Network	18
0.4.3	Convolutional Neural Networks	19
0.4.4	Implementation details	21
0.4.5	Dilated Convolutions	22
0.4.6	Focal Loss	23
0.4.7	Training Data	24
0.5	Results: Network Prediction for the String Location	24
0.6	Conclusion	30
0.7	Acknowledgement	31
0.8	Reference	32

0.1 Introduction

0.1.1 Cosmic Microwave background

CMB maps are the left over of big bang. We can see the CMB saturating space which began at about 378,000 years after the big bang. Before the creation of CMB the universe was hot,dense and plasma containing both matter and energy.Since lights are photons and at that time the photons could not move freely, no lights escaped earlier to that time. The universe had cooled to temperature of 2700 Celsius in Recombination era ,cool enough to recombine electron and photons to recombine into hydrogen atoms. Photons were released and this is today called the CMB. Photons were released and this is today called the CMB.The CMB confirms that the the overall Big Bang theory was correct.

This also provides insights on the composition of the universe.Such as the universe is made of dark energy about 68.3 percent, the mysterious force that is driving the expansion of the universe. Then the dark matter about 26.8 percent, which only interacts with the universe with the gravity. Normal matter like star,planets and galaxies makes up only 4.9 percent mass of the universe. Moreover, in the same way the CMB can also help us to identify the existence and location of cosmic string.

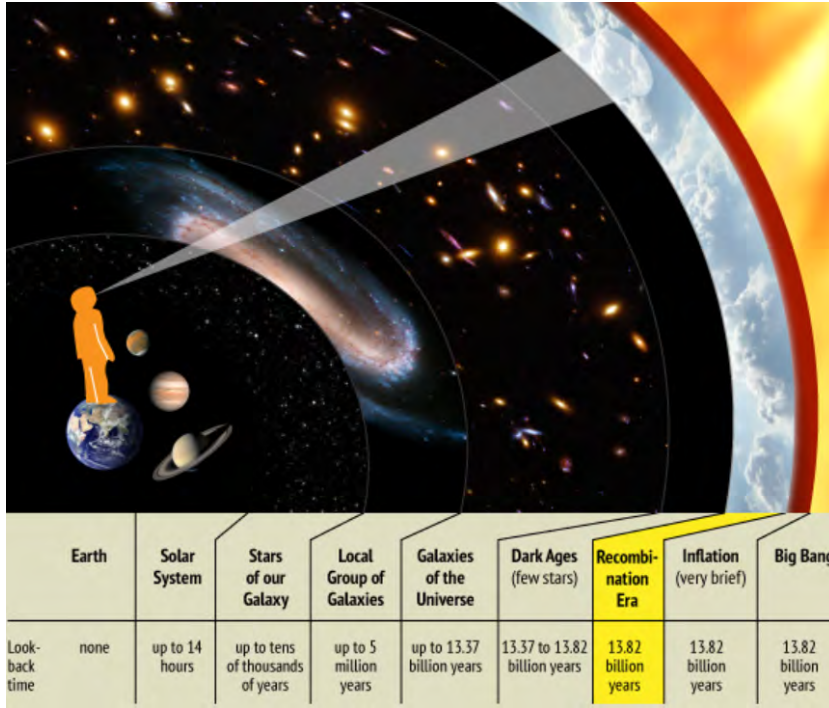


Figure : Explanation of the creation of CMB.

0.1.2 Cosmic String

Cosmic strings are formed in 10^{-34} s after the big bang. These strings are much thinner than proton but if they are of length of a kilometer they will be heavier than the mass of the earth. They are formed in the phase transition in the same way the Higgs field undergoes phase transition while it gives masses to the particle. So to define Cosmic strings are hypothetical 1-dimensional topological defects which may have formed during a symmetry breaking phase transition in the early universe when the topology of the vacuum manifold associated to this symmetry breaking was not simply connected. In this particular case while the phase transition happens(changes from one high energy to another),it doesn't happen so smoothly throughout the universe.

There are various part of the universe where the original part of the energy stay the same (the high energy bit gets trapped). These forms the line the long string(they are in the

high energy and surrounded but the new phase which has lower energy). When they are formed we have a long string's network crossing across the universe ,creating loops .Since they are so massive and so much tension they begin to flop around. As they flop around the speed of light or about the half the speed of light they begin to cross one another.

We can imagine the cross of string like a shoe lace as it wraps back and crosses itself with a shoe lace , we can't do anything it can not go through itself. But with a cosmic string they can go they chop off at that point where they crosses itself (break at junction). These loops of string are now under huge tension (huge mass and oscillating,moving closer at good fraction of speed of light). Since they are moving and oscillating they radiate gravitational waves. Just like any massive object that moves will radiate gravitational waves.

Gravitational waves is cosmic strings principle way of losing energy. Because if they didn't do that what would happen is the long strings would just keep stretching as the universe expands that will be like pulling an elastic band and the energy stored in this strings will get bigger and bigger and eventually they will dominate all the other energy contribution to the universe. That would completely change the dynamics of the universe and that doesn't happen we don't seen any. So either they are not there or something else happened which means they don't dominate.

Long strings forms loops and the loops can radiate the energy in gravitational waves . Then they can reach to a stable scaling solution where the energy stored in the strings becomes a constant fraction of the total energy of universe so it never comes to dominate (the energy in the strings doesn't disappear or grow big it just becomes constant, just right). That was where got people excited (the Goldilocks amount of energy).

Tom Kibble first first came up with this amazing idea of the formation of this objects. He demonstrated when they evolved under the expansion of the universe that they chop off

the loops and they would radiate away their energies in just the right amount so that the overall energy of network of strings would be some fixed fraction of the background energy. It turns out that we can work out the fixed fraction and we find it for phase transition which corresponds to what we call the grand unified phase transition (where we unify the strong, the electro-weak and electromagnetic forces that is about 10^{-35} after the big bang).

Energy scale associated with that which determines the masses of these strings is just sufficient to lead fluctuation in the matter that produces the cosmic microwave background radiation and the distribution of galaxies. From 1970's to 1996 this provided a belief that the cosmic strings are the seeds from which structures would be reconstructed.

Now there is another rival theory called the inflationary theory of universe. They are competing theory of cosmic string. Unfortunately cosmic microwave background image is becoming better and more accurate and we could see the fluctuation in the temperature of the microwave background all different size across the observable universe. We are beginning to fit our cosmic string prediction with what we observe in terms of what this distribution should be.

We found that cosmic string is not working since the predicted calculation were not matching with observed cosmic microwave background anisotropies. People began to lose interest for this theory. Although there are analogous objects observed in condensed matter system (liquid helium system, nematic liquid crystals). Also their scaling properties are all seen and matched what we might expect from cosmology there are not yet seen. There are numbers of condensed matter system which are driven by loops of vortices and effectively of strings. Such as a particular equation called the sine-Gordon equation which is used in helium.

0.1.3 Cosmic Super String

Back in the 1990's to the end of the 2000's people begin to lose interest these cosmic strings since there were not doing as they are said in the tin. Particularly when we look on the observed map; the power as a function the angle in the sky we are looking at also know as the Doppler peaks. This got a very distinctive set of peaks. We compare with the prediction of cosmic strings. The cosmic strings should give us only one peak not the secondary Doppler peaks.

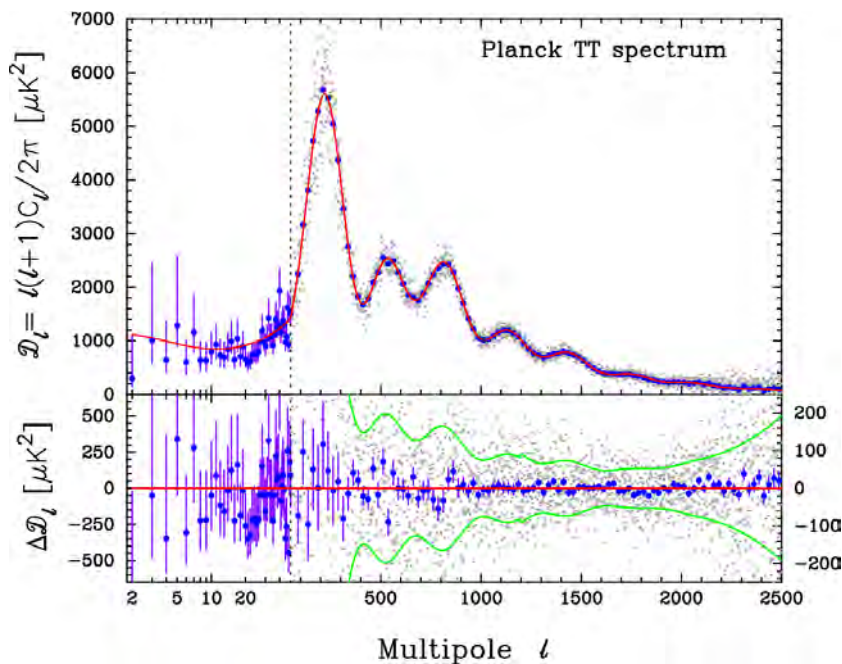


Figure: Doppler leaks from Planck 2013 data.

For a while people began to lose interest for cosmic string. Then the idea of super string comes. People became interested another type of string which they call the fundamental strings also known as super string of string theory. Ed.Witten asked the obvious question if we have cosmic strings and those fundamental strings may be they are the same thing. Ed.Witten came to the conclusion that it couldn't be the same thing. The fundamental string seemed very unstable. So if a fundamental string is formed that in a size of the galaxy. Then it should chop off incredibly quickly. Ed.Witten also discovered that if we

look at the natural value of the mass of the fundamental string it was way to big compared what observation was telling us the cosmic string could be. So the masses didn't work out , it was seemed it ,it won't work.

In the early 90's there happened to be a second type of String revolution. It was realized that a new class of object could formed. The normal string which we thought could not be stable. It could have mass per length(tension) way much less Ed.Witten had thought, it opened up possibility that, may be these strings could be like the cosmic strings which we call the cosmic super string. [E. Copeland, Dark Matter in the Universe 99 (1990).] This rejuvenated the subject. This new kind of string has some unusual property. They could come in different flavours. It's for simplicity one has orange and mango flavour.They would not pass through of each other. They can not simply chop. They would have to form a composite in between so it ended up with a position where those strings would no longer form simple loops. They the form so called junctions. A three way junctions. So two strings will come in and they hit each other. The point they hit each other that have to be a new bridge. So this led to this more complicated networks [1 . Ed.Copeland ,Kibble Strings and Super strings, 2009]. Physicists are looking at the possibilities that this objects could actually be seen not only in the microwave background and also the decay of gravitational waves. These strings and cosmic strings have some wonderful properties.

0.1.4 Cosmic string in String theory and QFT

Cosmic string can be interpreted by many theory both in string theory and quantum field theory. Like in theory of fundamental strings, in M strings or in D strings. As per[55,58],in string theory, the role of cosmic strings can be played by the fundamental strings (or F-strings) themselves that define the theory perturbatively, by D-strings which are related to the F-strings by weak-strong or so called S-duality, or higher-dimensional D-, NS- or

M-branes that are partially wrapped on compact cycles associated to extra spacetime dimensions so that only one non-compact dimension remains.

The prototypical example of a quantum field theory with cosmic strings is the Abelian Higgs model. The quantum field theory and string theory cosmic strings are expected to have many properties in common, but more research is needed to determine the precise distinguishing features. The F-strings for instance are fully quantum-mechanical and do not have a classical definition, whereas the field theory cosmic strings are almost exclusively treated classically.

Cosmic strings are really thin and extremely massive. Their width is described as zero width or NambuGoto approximation. So the cosmic string is like a line and obey the NambuGoto action, which is classically equivalent to the Polyakov.

In fact the width is set differently by different theories, The string width is set by the scale of the symmetry breaking phase transition, as per explanation of field theory. The string width is set (in the simplest cases) by the fundamental string scale, warp factors (associated to the space time curvature of an internal six-dimensional space time manifold) and/or the size of internal compact dimensions as per String theory. The universe is either 10- or 11-dimensional, depending on the strength of interactions and the curvature of space time as described in string theory .

0.1.5 Observation of Cosmic String

It is expected that at least one string per Hubble volume is formed. When we have a loop of cosmic string oscillating back and forth every now and again once in an oscillation usually there will be a part of the strings forming cusp. This cusp is very sharp region which

instantaneously goes at the speed of light. Since it is sharp, it has so much energy packed in the region that it can emit bursts of gravitational waves. There are detectors out there such as the LIGO detector ¹ and the upgraded advanced LIGO detector so these would detect the beaming events coming out of the strings. Many are working like Ed.Copeland on the properties of these beaming events so that to see whether or not they could be detected by these gravitational waves . These is one of the main things the LIGO detectors will be looking for,the beams of gravity. Which are shooting out from this objects .

Since cusp are so sharp they just don't bream gravitational waves they beam other things such as they can bream particles out. So they are like ultimate laser which can boom.The neat thing is that they are not doing it all the time, just once a cycle. It goes beaming and beaming like an pulsing effect that we can begin to look for,it's an distinctive signature. So we have those to detect cosmic string.

The other features on the strings which are called the kinks. Every time a string chops off it leaves this discontinuity. Where one string is coming and it meets the other string. In the point they have meet, a loop has gone off. We are left with this sort of discontinuity. A one string here and the other string there. They begins to propagate around the configuration which builds up kinks which also radiates. Which in turn creates extra beaming effect. Much effort has been given to understand the distribution of these things, the amount of the radiation and the rate of radiation. It is not seen yet. One interpretation of these is that if some thing is not seen it doesn't mean those things are not there instead it gives idea about the mass scale.

¹The Laser Inter-ferometer Gravitational-Wave Observatory (LIGO) is a large-scale physics experiment and observatory to detect cosmic gravitational waves and to develop gravitational-wave observations as an astronomical tool. Two large observatories were built in the United States with the aim of detecting gravitational waves by laser interferometry. These can detect a change in the 4 km mirror spacing of less than a ten-thousandth the charge diameter of a proton, equivalent to measuring the distance from Earth to Proxima Centauri (4.0208x10¹³km) with an accuracy smaller than the width of a human hair.

The mass scale should be low since it should be visible if the mass scale of the string is high enough. If mass scale was high then the tension in the string should be high that would beam more energetically and we would have seen them. Since the mass scale is dropping it is hard to reconcile them with grand unified theories although they are consistent with some of the cosmic super string model. So those are perfectly plausible. Despite the fact that CMB images are not matching, not finding those gravity laser or cusp, not finding any evidence and in fact some of those are against the theory. Physicist are still interested because firstly the idea of phase transition is well accepted in particle physics and the Higgs mechanism is a phase transition . Moreover the breaking of symmetry is going on is well accepted. What is more, these objects are seen in equivalent terrestrial system is an evidence. This tells us the idea is work.

Phase transition happened but whether or not it happened in such a way that they caused those topological defects are not confirmed. However there are different types of cosmological defects such as mono poles, domain walls and texture. These could have all formed, in fact mono poles is the reason behind the idea of inflation. This things comes so naturally that still efforts are given to search cosmic string. It is still interpreted on the bound of strings ,the reason why it is not yet observable. It may not not happen eventually when the detectors will fail completely but not at that stage.

In fact Planck² on 2013 second year of observation will be looking for polarization effect that's whether the radiation gets polarized by the presence of objects and cosmic strings can do that it can polarize the light. B-Modes is a particular type of polarization of light with magnetic fields is a signal of cosmic string. Ed. Copeland and many other are working on nature of the signature signal and trying to figure out if those signal are in the Planks data or not. The long string which are of the stretch across the observable universe should be of order 10^1 but they are chopped off continuously, so there would be billions of chopped off loops of strings. These loops then gradually decay. The majority of the loops are chopped off is around the size of observable universe at that time so there would be a long time to decay and they will be chopped off all the time. In that way there will be replacement of loops all the time. So a group will decay, a group will be decaying and a whole new group will begin.

Since the majority of the loops are self intersecting there will be the loops all the time. Some of them are not self intersecting. The non self intersecting loop match or have one to one map with the distribution of clusters of galaxies. Since they are so massive and thin, those are not observable in human eye. They will attract matter, so the surrounding objects will be attracted and since those travel three or four times faster than light that will make oscillation. The process and dynamics are formed to understand them makes complete sense. Those make them serious candidate for structures.

²Planck was a space observatory operated by the European Space Agency (ESA) from 2009 to 2013, which mapped the anisotropies of the cosmic microwave background (CMB) at microwave and infra-red frequencies, with high sensitivity and small angular resolution. Planck provided a major source of information relevant to several cosmological and astrophysical issues, such as testing theories of the early Universe and the origin of cosmic structure; as of 2013, it has provided the most accurate measurements of several key cosmological parameters, including the average density of ordinary matter and dark matter in the Universe. On 21 March 2013, the mission's first all-sky map of the cosmic microwave background was released, with an expanded release including polarization data in February 2015. The final papers by the Planck team are expected to be released in March 2018.[3]

0.2 Non-machine learning Approaches

Many geometrical edge detection algorithms are used in detecting cosmic string. Among them are curve let, wavelet and canny are the most used. Most of the detection algorithm search for the GKS(Gott-Kaiser-Stebbins) effect. When an string move between observer and the surface of last scattering, it makes an step discontinuity. That is the GKS effect. When we look for this effect in the WMAP data it gives null detection and a limit of $G_\mu < 1.5 \times 10^{-6}$. Another way to detect cosmic string is though the emission of the gravitational waves such as from cusp and kinks.

The CMB angular power spectrum on the WMAP data gives a constraint an order of magnitude higher than that from the GKS effect. The strongest constraint is constructed from the Plank Collaboration. They made the upper bound on the string tension for Nambu-Goto strings of $G_\mu < 1.3 \times 10^{-7}$ at the 95 percent confidence level.

The actual limits of detection provided by Canny are for string tension above $G_\mu = 10^{-6}$. With a lot of false positive or extra edges. This limit of tension is even higher when there is noise in the data. Curve let can detect for $G_\mu = 1.4 \times 10^{-6}$ and even more vulnerable to noise. Another Edge detection algorithm which has been discussed in [31,34] is the wavelet. Wavelet can detect cosmic string with tension $G_\mu = 5 \times 10^{-6}$.

Using pulsar timing constraints, the North American Nanohertz Observatory for Gravitational Waves (NANOgrav) places limits of $G_\mu < 3.3 \times 10^{-8}$ at the 95 percent confidence level [23]. Joint interferometer experiments such as the LIGO-Virgo Collaboration are also searching for the gravity wave background from loops [24, 25] and cusps. Much of the work is going on to understand the way to detect the kinks. References [31,33] used the Canny algorithm to detect GKS edges made from long strings in the CMB temperature

maps simulated with this model. They found more short edges in maps with strings which they interpreted as the disruption of long edges by Gaussian noise[36]. So none of the Edge detection algorithm works when there is much Gaussian noise.

Since a lot of fine CMB maps are coming ,the search for cosmic string is getting a more exciting field of research day by day. In 21 cm red-shift surveys we could observe cosmic strings wakes through their distinctive shape in red-shift space [17,21] or by using the correlation between CMB and 21-cm radiation from dark ages [22]. Machine learning approaches has several advantages over the non-machine learning approaches. Those Algorithm learns the features by themselves. While non machine learning approaches has to be given the prior knowledge as shapes. In case of noise none of the edge detection algorithm will work as good as the machine learning approaches since machine learning is statistical generalization not memorization. We can explain the behaviour of edge detection algorithm with noise as over-fitting in data science.

The disadvantages of using machine learning techniques is that they require a lot of data to train with a lot of computational resources. Moreover, in this cosmic string search scenario requires a lot of simulated data to be made and the simulation takes a lot of computational resources. Fortunately in the recent time, as the development of powerful GPU which supports faster parallel computation, the simulation for data set as well as the training is now possible with complex learning architecture. So the main benefit of using non-machine learning algorithm , that it requires less computational resources with the price of accuracy is not a big advantage now a days. Moreover, Canny and Canny-like edge detection algorithm can not find cosmic string location properly on the sky map which is a huge disadvantage.

Despite this disadvantages, Canny ,wavelet and curvelet analysis has a lot of room to exploration and improvement.Since they require a statistical measure to identify the differ-

ence in number of edges between a sky map with strings and without string much like a objective function in machine leaning , lots of fine tuning can be done to improve the result while using those edge detection algorithms.

0.3 Machine Learning Approach

Bayesian interpretation of cosmic string detection improves two major goals: 1)it unifies all the previous models and have mechanism to unify new approaches and make a non-uniformly learn able hypothesis which makes it easy to figure out a optimal hypothesis for cosmic string search. 2)It also derives a linkage between the cosmic string location and cosmic string tension G_μ . It presented a framework within the context of detection of cosmic string through GKS effect on the CMB temperature entropy maps. However ,it could be equally applied to 21cm intensity maps to detect cosmic string. ³

From our perspective a single string produces a signal which is localized in position space so only the neighbouring pixels are affected. However,Fourier representation of a string cause all the models to change. This makes extremely hard to identify if a pixel belongs to cosmic string or not. Identifying location of cosmic string is important since it helps to to further investigate on the concentrated area.

³In cosmology, intensity mapping is an observational technique for surveying the large-scale structure of the universe by using the integrated radio emission from unresolved gas clouds. In its most common variant, 21 cm intensity mapping, the 21cm emission line of neutral hydrogen is used to trace the gas. The hydrogen follows fluctuations in the underlying cosmic density field, with regions of higher density giving rise to a higher intensity of emission. Intensity fluctuations can therefore be used to reconstruct the power spectrum of matter fluctuations. The frequency of the emission line is red shifted by the expansion of the Universe, so by using radio receivers that cover a wide frequency band, one can detect this signal as a function of red shift, and thus cosmic time. This is similar in principle to a galaxy red shift survey, with the important distinction that galaxies do not need to be individually detected and measured, making intensity mapping a considerably faster method.Source:Wikipedia

The approach currently used in cosmic string detection is by taking the entire sky map and estimate G_μ from it. However the machine learning approaches we are proposing take the sky map and produce another map with probabilistic estimates of string locations. From that map we estimate G_μ . The second step used to estimate G_μ is straight forward whose input is the map of probabilities produced by the neural network. Splitting G_μ in that following way gives two advantages :1)the likely information of the location of cosmic string on the sky. 2)Sample complexity for a neural network is much less then to learn to produce a map of cosmic string location then what would require for a Artificial Neural Network to produce an estimate of G_μ from the sky map. The reason behind this is that string effects are highly local and produces one training sample per pixel, instead of one training sample per full map. Therefore machine learning approach are much better suited to produce the string location map instead of directly estimating G_μ . This process split up the problem into two halves 1)produce a probabilistic string map(using machine learning) 2)calculate G_μ from a map of probability (something human can do well).

In the context of machine leaning this is a supervised problem. We need to classify if a pixels belongs to a string or does not belong to a string. The mechanism we are using to classify is a dilated convolutional neural network with focal loss. We implemented it with a convolutional neural network trained on simulations of CMB anisotropy maps with and without strings and used it to estimate string locations on a CMB sky temperature map.

In the next section we present a Bayesian point of view which focuses on obtaining $P(G_\mu|\delta_{sky})$,the probability distribution of string tension G_μ given a sky map δ_{sky} . It has been done by out-ling a procedure to estimate the string locations in the sky given a sky map and deriving an expression for $P(G_\mu|\delta_{sky})$ which uses information about string locations maps. In section 8 how machine learning can be used to produce probabilistic string location and in the process optimization of cosmic string in CMB sky map is discussed. Then how machine learning with a neural network can be implemented is discussed. Then our results

are compared with previous works to predict location of cosmic strings. It is found on the work that accurately predict the value of the string tension on simulated maps with a G_μ as low as 4×10^{-9} .

0.4 Neural Network prediction for String Location

0.4.1 Supervised Learning

The supervised learning problem seeks to assign labels to data points given a data set of examples pairs. Suppose we have a data set $D = \{x_i, y_i | i = 1 \dots N\}$, where x_i and y_i are the data points.

Casting the problem of prediction string location a $m \times m$ pixels CMB map as a supervised learning problem, we make the following assignment: $A = R^{m \times m}, B = 0, 1^{m \times m}$, the data set $D_{train} = \{(\delta_{sky}^i, \xi^i) | i = 1 \dots N\}$ is made up of N simulated sky temperature maps, δ_{sky}^i , at different G_μ and the associated string location maps ζ^i . Given a pixel $j = (j_1, j_2)$, $\zeta_{sky}^i \equiv 1$ or 0 , depends on whether a string is located at the pixel or not. In this context

$$f_w \equiv \prod_{j \in pixels} (f_{w,j})^{\xi_j^i} (1 - f_{w,j})^{1 - \xi_j^i}$$

is a convolutional neural network, to be desired. with free parameters labeled by w and finally the error function used is the cross-entropy,

$$E(w) = \sum_{\delta_{sky}^i \in D_{train}} \sum_{j \in pixels}$$

Then we used focal loss discussed later.

0.4.2 Neural Network

Neural networks are multi-layered [46] functions that approximate a desired function. It has some weight vectors to parameter. We can define a hypothesis class consisting of neural network predictors, where all hypothesis share the underlying graph structure of the network and differ in the weights over the edges. It can be shown that every predictor over n variables that can be implemented in $T(n)$ can also be expressed as a neural network predictor of size $O(T(n)^2)$, [42] where the size of the network is the number of nodes in it.

Feed forward network are a class of neural network whose underlying graph does not contain cycles. A feedforward neural network is described as directed acyclic graph, $G=(V,E)$ and a weight function over the edges, $w : E \rightarrow R$. A simple 1 layered example of such a form with h_1 "hidden units" which maps from R^{nm} is $F(x) = W^2\sigma(W^1x + b^1) + b^2$.

In general $F_{mlp} = F_n(F_{n-1}(\dots F_1(x; w_1)\dots; w_{n-1}); w_n)$ The ERM(Empirical Risk Minimization) process is minimizing the objective function $E(W) = \sum_i^N ||y_i - F_{mlp}(x_i; W)||$. We can use least square norm or cross entropy for that. For mulilayered function F , the error landscape is in general non-convex and has multiple local minima. Through non-trivial, it is nonetheless possible to optimize using various algorithms but most most of them uses the gradient descent approach. Back propagation algorithm is used to perform gradient decent.

Casting the problem of prediction string locations on an $m \times m$ pixels CMB map as a supervised learning problem, we make the following assignment:

$$A = R^{m \times m}, B = 0, 1^{m \times m}.$$

The data set $D_{train} = (\delta_{sky}^i, \zeta^i)_{i=1 \dots N}$ is made up of N simulated sky entropy, δ_{sky}^i , at different G_μ and the associated string location ζ^i .

0.4.3 Convolutional Neural Networks

Convolution neural network are special type of neural network specialized in processing data and learning from it. This has a grid like topology. In most general[45], the convolution is an operation on two functions of a real valued argument $s(t) = \int x(a)w(t - 1)da$, that is, $s(t) = (x * w)(t)$

In machine learning terminology the first argument (the function x) to the convolution is referred as input and the second argument as the kernel. The output is referred as feature maps[39].

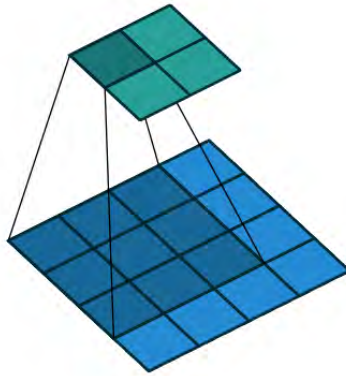


Figure 1: A convolution of a 2×2 kernel on a 4×4 image[49]

In practice, for a kernel \mathbf{k} , input \mathbf{x} , and output \mathbf{x}' the convolution can be expressed as

$$x'_{i,j} = b + \sum_{u=1}^{k_h} \sum_{v=1}^{k_w} x_{i',j'} k_{u,v} \quad \text{with} \quad \begin{cases} i' = i \cdot s_h + i + s_h + u - 1 \\ j' = j \cdot s_w + j + s_w + v - 1 \end{cases} \quad (1)$$

where \mathbf{k} is a matrix of weights, the kernel, k_h and k_w are the height and width of the matrix, s_h and s_w are the strides of the kernel on the height and width, and b is a bias

term. The bias term b and the parameters of the kernel matrix \mathbf{k} are free parameters.

In contrast with the previous section, which transformed data stored in a vector into another vector, convolutions transform data stored on a matrix into another matrix. They have two unique properties that make them particularly well suited for image data.

- Each component in the output is produced from a function with only the elements in the kernel centered on the component location on the previous layer, encouraging it to build low level spatial feature detectors to progressively build higher level feature detectors
- The kernel has shared weights for all locations across the image; this allows it to act identical to classical image processing methods, such as the Sobel Edge Detection filters, but with learned parameters.

For the more general case with \mathbf{x} having multiple input channels, and \mathbf{x}' having multiple output channels, and both being represented by 3D tensors, the above equation applies with the more general form:

$$x'_{i,j,k} = b_k + \sum_{u=1}^{W_h} \sum_{v=1}^{W_w} \sum_{f=1}^{W_d} x_{i',j',f} W_{u,v,f,k}$$

$$\text{with } \begin{cases} i' = i \cdot s_h + i + s_h + u - 1 \\ j' = j \cdot s_w + j + s_w + v - 1 \end{cases} \quad (2)$$

where \mathbf{W} is a generalized weight tensor, W_h , W_w and W_d are the height and width and number of channels of the weight tensor, respectively, f is the number of input channels, k is the number of output channels.

```

1  from keras.models import Model
2  from keras.layers import Input, Dense, Conv2D
3  import numpy as np
4
5  def modelcreate():
6      filter_length = 32
7      kernel_size = 3
8
9      final_kernel_size = 1
10     final_filter_length = 1
11
12     inputs = Input(shape=(512, 512, 1))
13     l1 = Conv2D(filters=filter_length, kernel_size=kernel_size, strides=1,
14               padding='same', activation='tanh', use_bias=True)(inputs)
15     l2 = Conv2D(filters=filter_length, kernel_size=kernel_size, strides=1,
16               padding='same', activation='tanh', use_bias=True)(l1)
17     l3 = Conv2D(filters=filter_length, kernel_size=kernel_size, strides=1,
18               padding='same', activation='tanh', use_bias=True)(l2)
19     l4 = Conv2D(filters=filter_length, kernel_size=kernel_size, strides=1,
20               padding='same', activation='tanh', use_bias=True)(l3)
21
22     model = Model(inputs=inputs, outputs=l5)
23     # no need to directly alter Adam as default parameters were used.
24     model.compile(optimizer='Adam', loss='binary_crossentropy', metrics=['accuracy'])
25
26     return model

```

0.4.4 Implementation details

We use a 4 layered Convolutional Neural Network introduced in [36], with the weight tensor for each layer being defined by W^a , where $a = 1, 2, 3, 4$, between maps of pixel size 512×512 . As we process black and white images, $W_d^1 = 1$, and $W_d^a = 32$ for all other values of a . We also define a bias vector b_a , where $a = 1, 2, 3, 4$ (one for each layer), with each vector having dimension 32.

This can be interpreted as defining a neural network where each layer (except the first) takes in a map with 32 channels, that is, vector dimension 32, and outputs a map with 32 channels, that is, vector dimension 32.

The map $(\mathbf{W}^1 * \delta_{sky} + \mathbf{b}^1)$ is a map with the same size as its input, 512×512 . By applying a non-linearity element-wise (we use tanh), the output $\mathbf{x}_1 = \tanh(\mathbf{W}^1 * \delta_{sky} + \mathbf{b}^1)$ is still a map of size 512×512 . By applying the four convolutional layers, we get:

$$\mathbf{x}_4 = \tanh(\mathbf{W}^4 * \tanh(\mathbf{W}^3 * \tanh(\mathbf{W}^2 * \tanh(\mathbf{W}^1 * \delta_{sky} + \mathbf{b}^1) + \mathbf{b}^2) + \mathbf{b}^3) + \mathbf{b}^4)$$

We then take the element-wise dot product at each pixel location with the vector \vec{c} (whose components are learned), producing a scalar pixel value at each pixel location on the image. We then add a scalar bias b_5 to each pixel location, and apply an elementwise sigmoid nonlinearity. Hence,

$$f_{w,\mathbf{j}}(\delta_{sky}) \equiv \text{sigmoid}(\vec{c} \cdot \mathbf{x}_4 + b_5)[\mathbf{j}]$$

We use the sigmoid function as it allows us to interpret the output map as probabilities that a string exists on a particular pixel, for which the values must be in the range (0, 1).

0.4.5 Dilated Convolutions

”Dilated” (or ”atrous”) convolutions[54] are often used as a computationally cheap method of increasing the receptive field of a kernel, allowing it to effectively compute higher level features without the computational cost associated with a larger filter. It does so by ”inflating” the kernel, by inserting spaces between kernel elements[49]. Along with the kernel size, a new hyperparameter, the dilation rate is introduced, which controls the spaces between the kernel elements:

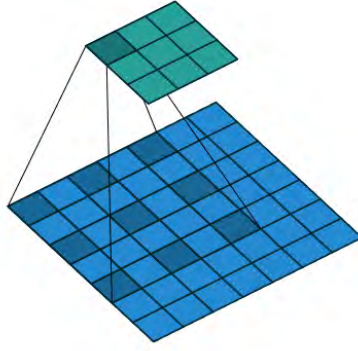


Figure 2: A convolution of a 3×3 dilated kernel on a 7×7 image, with dilation factor 2[49]

If the dilation factor is d , the convolution operation can be expressed as:

$$x'_{i,j,k} = b_k + \sum_{u=1}^{\lfloor W_h/d \rfloor} \sum_{v=1}^{\lfloor W_w/d \rfloor} \sum_{f=1}^{W_d} x_{i',j',f} W_{u,v,f,k}$$

$$\text{with } \begin{cases} i' = i \cdot s_h + i - s_h + u \cdot d - d \\ j' = j \cdot s_w + j - s_w + v \cdot d - d \end{cases} \quad (3)$$

For testing a version of the convolutional neural network with dilated convolutions, we simply take the network detailed in Section 10.4, and replace the standard convolutions therein with dilated convolutions, appropriately padding the input where necessary.

0.4.6 Focal Loss

The standard loss used to train a model like this is a per-pixel cross entropy loss, where, if for notational convenience,

$$p_t = \begin{cases} p & \text{if } y = 1 \\ 1 - p & \text{otherwise} \end{cases} \quad (4)$$

then the cross-entropy loss is,

$$\text{CE}(p_t) = -\log(p_t)$$

Focal loss, introduced in[54], modifies the above crossentropy loss with a modulating

factor $(1 - p_t)^\beta$, down-weighting easy samples, and focusing the training on hard negatives. Focal loss can then be defined as:

$$\text{FL}(p_t) = -(1 - p_t)^\beta \log(p_t)$$

We hypothesized this loss function to be particularly relevant to the context of cosmic string detection, as there are many easy negatives, but the hard negatives are the ones the model fails to classify properly, resulting in increased false positives. We hoped this modified loss would reduce the number of false positives further.

0.4.7 Training Data

Our model will be trained on the data set in a similar fashion to [53] on numerically generated CMB temperature maps with and without cosmic string. Which is generated using the same long string analytical model[35]. To test the performance of our model we used data augmentation on a few CMB to generate a dummy training set.

0.5 Results: Network Prediction for the String Location

We used Keras with Tensorflow background to train our model. Our model will be made up of 512×512 pixels with a resolution of 1 arc minute per pixel. This leads to sky map showed in Fig 1a. For values of the string tension we will study $G_\mu \leq 10^{-7}$. However pure Gaussian map with G_μ is indistinguishable by eye with the one that has $G_\mu \leq 10^{-7}$. One of the unknown value between 1 and 10 is the number of strings per Hubble volume, N_H . We first trained our neural network with a value of $N_H=1$.

We believe, this did not impair the predictive power for input maps with larger N_H values. Then we nested the robustness of our model by adding a few white component. In the realistic case there would be a lot more noise. Below we highlight results which confirm the

soundness and power of the Bayesian machine learning framework and its neural network implementation, that we have presented in [53] and tried to argue why our model will perform even better.

we show neural network predictions for the string location map using different values for $G\mu$, with $N_H = 3$, and no noise from [53] in figure 2. Here, the shades of grey in the string answer map correspond to the relative strength of the strings GKS temperature discontinuity.

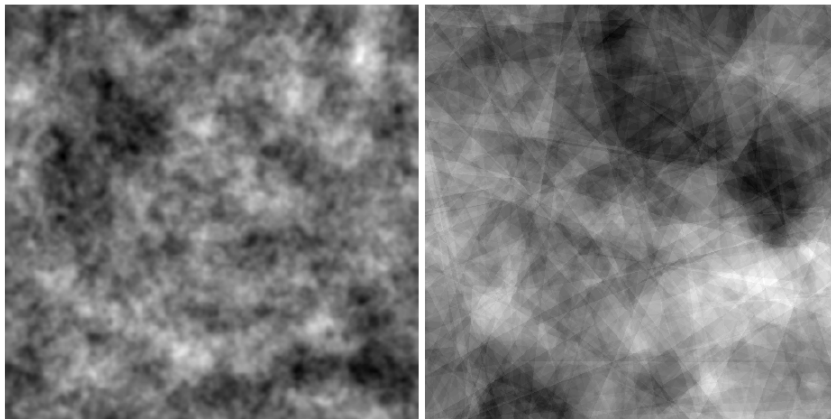


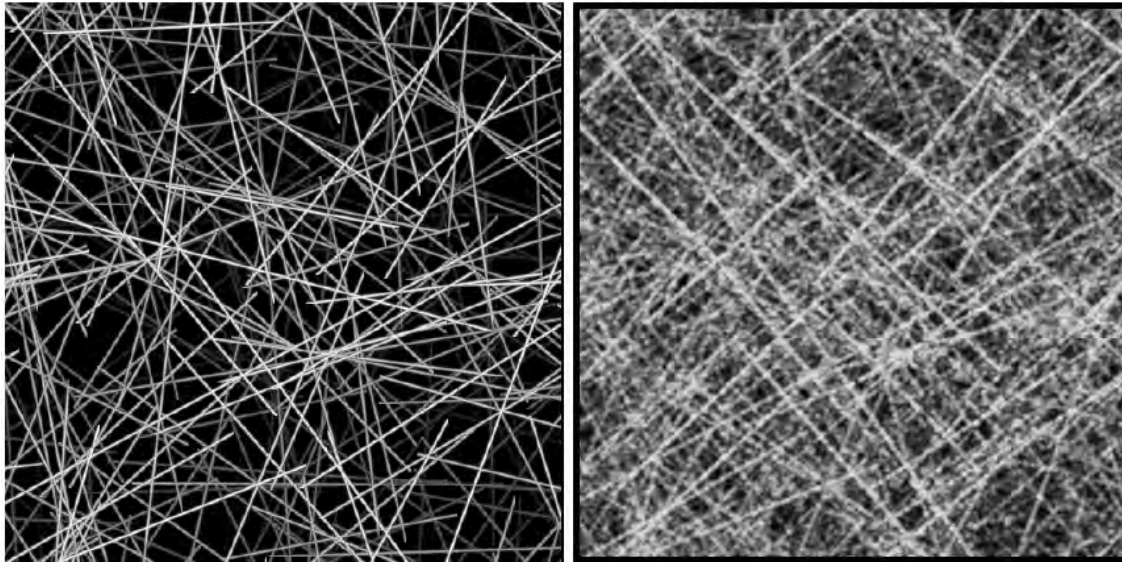
Figure 1: CMB anisotropy temperature maps of 512×512 pixels with a resolution of 1 arcminute per pixel.

(a) The full sky map, δ_{sky} . The white and black pixels are $+450K\mu k$ and $-450\mu K$ anisotropies, respectively. However, Maps with and without strings are indistinguishable by eye.

(b) String component δ_{string} to the full sky map.

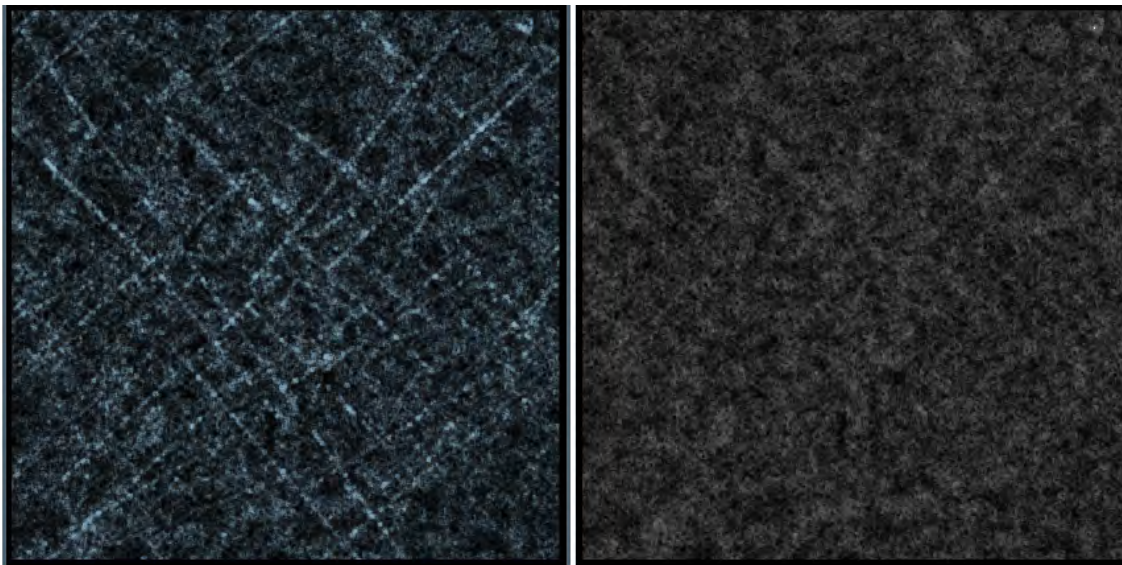
The shades of grey in the prediction maps correspond to the probability of a pixel being on a string. Completely black pixels are probability 0 and completely white pixels are probability 1 of being on a string. As $G\mu$ tends to zero, the neural network provides less information of whether a pixel is on a string or not and the pixel probabilities tend to the

prior $P((i; j) \in \text{string})$ which is given by the number of pixels on strings in the Answer map (Fig. 2a) divided by the total number of pixels. Thus as G_μ tends to zero, prediction map will become more uniformly grey, as 2d shows for [53]. But our neural network with dilated CNN performs even better with less G_μ .



(a) Map of strings used in the simulation

(b) Prediction when $G_\mu = 10^{-7}$



(c) Prediction when $G_\mu = 10^{-8}$

(d) Prediction when $G_\mu = 5 \times 10^{-9}$

Figure 2: Neural Network Predictions Without Noise. All the figures correspond to 512×512 pixels with a resolution of 1 arcminute per pixel. In 2a we show our answer map,

i.e. the actual placement of long strings in our patch of sky for $NH = 3$. In 2b, 2c, 2d, 2e(dilated CNN with focal loss) we show neural networks prediction of ξ for different value of the string tension with no noise. The shades of grey of the strings in the string answer map correspond to the relative strength of the strings GKS temperature discontinuity. The shades of grey in the prediction maps correspond to the probability of a pixel being on a string, with completely black pixels being 0 probability and completely white pixels being probability 1.

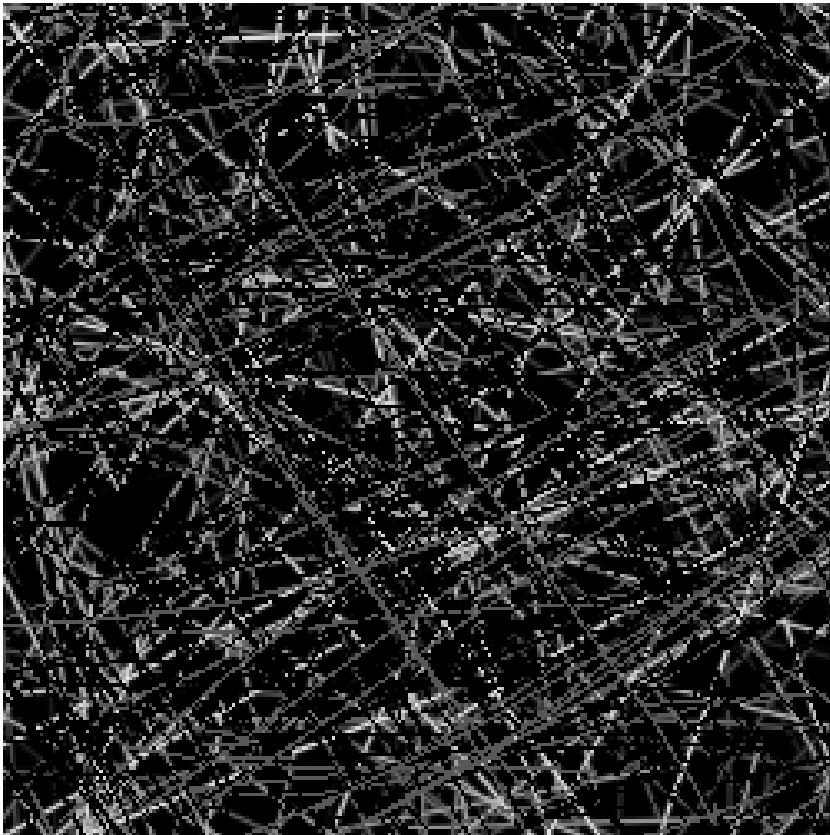


Figure:2e.Prediction with focal loss ($G_\mu = 10^{-9}$)

Looking at Fig. 2, we see that we can reconstruct string locations by eye at $G \approx 10^{-8}$. To compare our results with the wavelet curvelet of ref. [34] look at their figure 3 and 5 for $\mu = 10^{-7}$. Their neural network predictions produces string location maps comparable to their figure 3 and 5 but for a string tension G_μ an order of magnitude lower. We now

compare in more detail Their neural network predictions, with the results obtained by using the Canny algorithm.

As per [53] stated Canny can only distinguish between strings and no strings for a $G_\mu \leq 10^{-7}$ [36] and when noise is included this drops to $G_\mu \leq 10^{-6}$.. These limits are similar to those obtained in [34]. We present their Canny edge maps in Fig. 3. The pure Gaussian, no string edge map is given in Fig. 3a, and those for string tension $G_\mu = 10$ and 10^{-7} in Fig. 3b and Fig. 3c, respectively. Fig. 3d shows only those edges that appear in the $G_\mu = 10^{-7}$ map of Fig. 3c but not in the no string map of Fig. 3a. The Canny edge maps in Fig. 3 are produced with the same procedure described in ref. [32,34]. In particular see figure 5 in [34] and figures 13, 14 and 15 in [34].

As explained in [31,33], Canny is used to distinguish between maps with and without strings by looking for an excess number of short edges (a few pixels or less) over the entire map. This can be noted by looking at Fig. 3d where we show those excess edges that appear as in a CMB temperature map with $G_\mu = 10^{-7}$. There are hundreds of short edges comprising of 1862 pixels out of the entire 512×512 pixel map. This is interpreted as the long edges due to strings being disrupted by the Gaussian noise. However the extra short edges found by Canny do not necessarily correspond to string locations as per explained in [54]. So our networking is performing better though with low confidence because of data set. Once we can make the perfect simulation to generate the data set the confidence will raise exponentially.

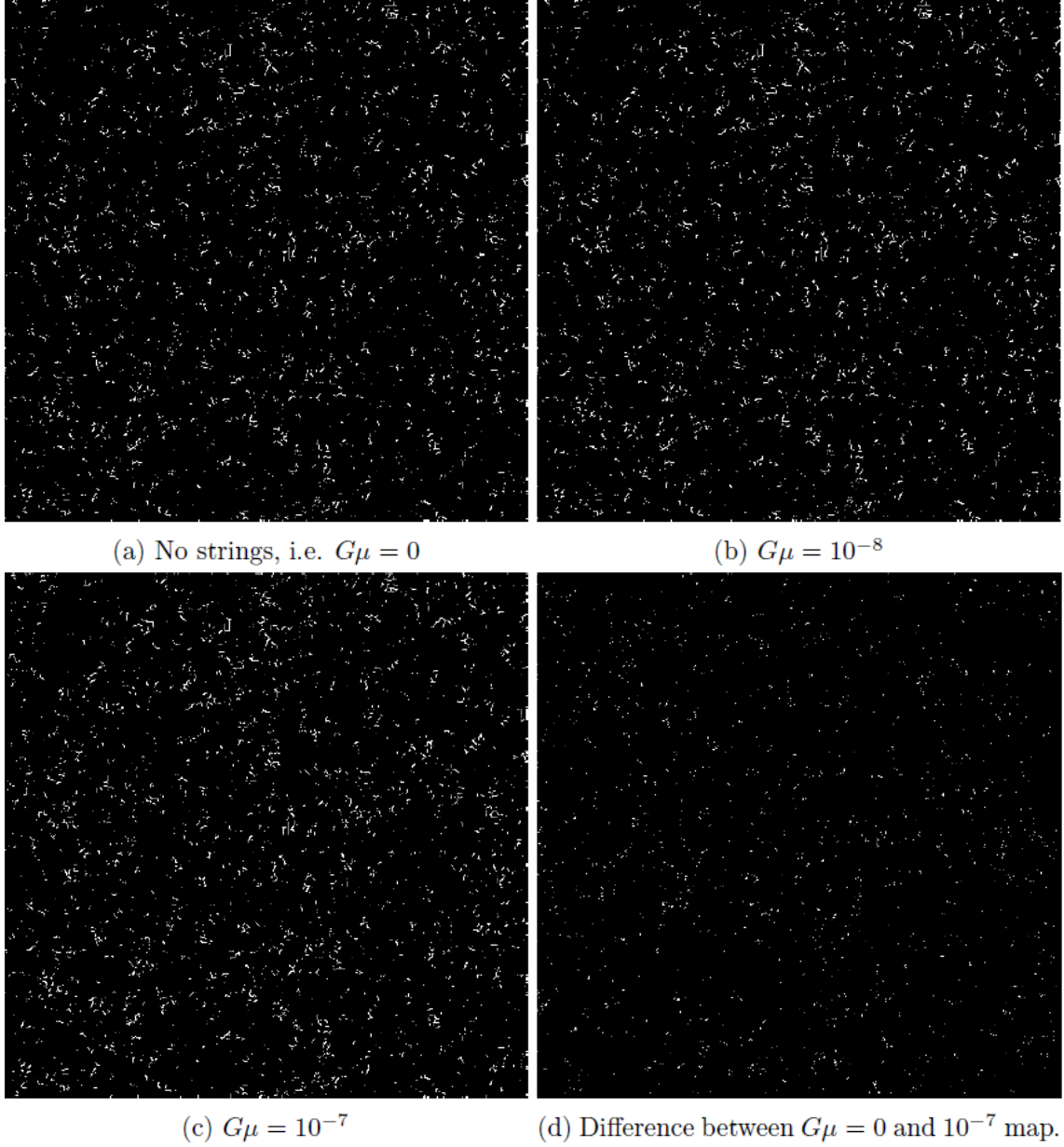


Figure 3: Canny Edge Detection Without Noise. All the figures correspond to 512×512 pixels with a resolution of 1 arcminute per pixel. In 3a we show the Canny edge map of pure Gaussian fluctuations without strings. Figures 3b and 3c show the Canny edge map with $G_\mu = 10^{-8}$ and 10^{-7} , respectively. The true string locations for these maps are given in Fig. 2a. Fig. 3d shows only those edges that appear in the $G_\mu = 10^{-7}$ map Fig. 3c but not in the no string map Fig. 3a. The edges in Fig. 3d occupy 1862 of the 512×512 pixels.

Results			
model	G_μ	Number of pixels cor- responding to string pixels	True positive rate
Canny	1×10^{-7}	310	17%
CNN	1×10^{-7}	1117	60%
CNN	1×10^{-8}	1060	57%
CNN	5×10^{-9}	423	23%
DCNN(Focal)	5×10^{-9}	965	88%
CNN	1×10^{-9}	243	13%
RPN	1×10^{-9}	698	65%
DCNN(Focal)	1×10^{-9}	779	74%

0.6 Conclusion

This project is an on going project. The model has quite good accuracy on our augmented data set. The confidence of the model will depend on the simulation used to produce the data set. Since the simulation for creating the data set is not finished the model has low confidence. Only two institute have the perfect simulation code and it take significant amount of computational capabilities to run the simulation. So far we are used data augmentation to create a pretty Small data set from very few images. Our next step will be to make a perfect simulation which will give higher confidence. Work has already on the way to do that. So the the earlier results are very promising.

The model can be used to detect string wakes in cm cm intensity maps and so many other cosmic objects. While applying this frame wok to 21 cm intensity map will require modifying the network presented here.

Our future plan is to consider realistic string simulation with noise similar to those simu-

lations discussed in [50]. Once noise is added more sophisticated network be to detect the string. From our point of view there is great possibility for improvement of the framework proposed here both by using better architecture here presented in as [51] or using deep reinforcement learning or goal based learning .

Now a days the general trends in deep learning research has been to improve performance with deeper network. Such as Google-Net which are used for object classification, image segmentation and evaluating Go board positions have order of 10^2 layers and 10^7 parameters. Training such network requires huge computational capability. So our plan is to use deep reinforcement learning with many layer to get better performance. Currently both for simulation to create the data set and training the framework with deeper layer both requires a lot of computational resources. So our main challenge now is to access such computational resources.

0.7 Acknowledgement

I would like to acknowledge the support of Irhum Shafkat from Rajuk Uttara Model College. I thank him for useful discussion and suggestions. The numerical simulation for creating the data set will be carried at the computer cluster of the Independent University (CCSE) and of the BRAC University (CVIS) jointly. Same resources will be used to train finalized deep models.

0.8 Reference

1. J. Magueijo, A. Albrecht, D. Coulson and P. Ferreira, Doppler peaks from active perturbations, *Phys. Rev. Lett.* 76, 2617 (1996) [arXiv:astro-ph/9511042].
2. U. L. Pen, U. Seljak and N. Turok, Power spectra in global defect theories of cosmic structure formation, *Phys. Rev. Lett.* 79, 1611 (1997) [arXiv:astro-ph/9704165].
3. R. Jeannerot, A Supersymmetric SO(10) Model with Inflation and Cosmic Strings, *Phys. Rev. D* 53, 5426 (1996) [arXiv:hep-ph/9509365].
4. R. Jeannerot, J. Rocher and M. Sakellariadou, How generic is cosmic string formation in SUSY GUTs, *Phys. Rev. D* 68, 103514 (2003) [arXiv:hep-ph/0308134].
5. S. Sarangi and S. H. H. Tye, Cosmic string production towards the end of brane inflation, *Phys. Lett. B* 536, 185 (2002) [arXiv:hep-th/0204074].
6. E. J. Copeland, R. C. Myers and J. Polchinski, Cosmic F- and D-strings, *JHEP* 0406, 013 (2004) [arXiv:hep-th/0312067].
7. R. H. Brandenberger, String Gas Cosmology, arXiv:0808.0746 [hep-th].
8. R. H. Brandenberger, Probing Particle Physics from Top Down with Cosmic Strings, *Universe* 1, no. 4, 6 (2013) [arXiv:1401.4619 [astro-ph.CO]].
9. J. R. Gott, III, Gravitational lensing effects of vacuum strings: Exact solutions, *Astrophys. J.* 288, 422 (1985). doi:10.1086/162808
10. N. Kaiser and A. Stebbins, Microwave Anisotropy Due to Cosmic Strings, *Nature*

310, 391 (1984). doi:10.1038/310391a0

11. A. S. Lo and E. L. Wright, Signatures of cosmic strings in the cosmic microwave background, astro-ph/0503120.

12. E. Jeong and G. F. Smoot, Search for cosmic strings in CMB anisotropies, Astrophys. J. 624, 21 (2005) doi:10.1086/428921 [astro-ph/0406432].

13. E. Jeong and G. F. Smoot, Validity of Cosmic String Pattern Search with Cosmic Microwave Background, Astrophys. J. 661, L1 (2007) doi:10.1086/518556 [astro-ph/0612706].

14. E. Jeong, C. Baccigalupi and G. F. Smoot, Probing Cosmic Strings with Satellite CMB measurements, JCAP 1009, 018 (2010) doi:10.1088/1475-7516/2010/09/018 [arXiv:1004.1046 [astro-ph.CO]].

15. C. Dvorkin, M. Wyman and W. Hu, Cosmic String constraints from WMAP and the South Pole Telescope, Phys. Rev. D 84, 123519 (2011) [arXiv:1109.4947 [astro-ph.CO]].

16. P. A. R. Ade et al. [Planck Collaboration], Planck 2013 results. XXV. Searches for cosmic strings and other topological defects, arXiv:1303.5085 [astro-ph.CO].

17. R. H. Brandenberger, R. J. Danos, O. F. Hernandez and G. P. Holder, The 21 cm Signature of Cosmic String Wakes, JCAP 1012, 028 (2010) [arXiv:1006.2514 [astro-ph.CO]].

18. O. F. Hernandez, Y. Wang, R. Brandenberger and J. Fong, Angular 21 cm Power Spectrum of a Scaling Distribution of Cosmic String Wakes, JCAP 1108, 014 (2011) [arXiv:1104.3337 [astro-ph.CO]].

19. O. F. Hernandez and R. H. Brandenberger, The 21 cm Signature of Shock Heated and Diuse Cosmic String Wakes, JCAP 1207, 032 (2012) [arXiv:1203.2307 [astro-ph.CO]].
20. O. F. Hernandez, Phys. Rev. D 90, no. 12, 123504 (2014)
doi:10.1103/PhysRevD.90.123504 [arXiv:1403.7522 [astro-ph.CO]].
21. R. H. Brandenberger, O. F. Hernandez and D. C. N. da Cunha, Disruption of Cosmic String Wakes by Gaussian Fluctuations, arXiv:1508.02317 [astro-ph.CO].
22. A. Berndsen, L. Pogosian and M. Wyman, Correlations between 21 cm Radiation and the CMB from Active Sources, Mon. Not. Roy. Astron. Soc. 407, 1116 (2010)doi:10.1111/j.1365-2966.2010.16951.x[arXiv:1003.2214 [astro-ph.CO]].
23. Z. Arzoumanian et al. [NANOGrav Collaboration], The NANOGrav Nine-year Data Set: Limits on the Isotropic Stochastic Gravitational Wave Background, Astrophys. J. 821, no. 1, 13 (2016) doi:10.3847/0004-637X/821/1/13 [arXiv:1508.03024 [astro-ph.GA]].
24. J. Aasi, J. Abadie, B. P. Abbott, R. Abbott, T. Abbott, M. R. Abernathy, T. Accadia and F. Acernese et al., Constraints on cosmic strings from the LIGO-Virgo gravitational-wave detectors, Phys. Rev. Lett. 112, 131101
25. B. P. Abbott et al. [LIGO Scientific and VIRGO Collaborations], An Upper Limit on the Stochastic Gravitational-Wave Background of Cosmological Origin, Nature 460, 990 (2009) [arXiv:0910.5772 [astro-ph.CO]].
26. C. Ringeval, M. Sakellariadou and F. Bouchet, JCAP 0702, 023 (2007) doi:10.1088/1475-7516/2007/02/023 [astro-ph/0511646].

27. L. Lorenz, C. Ringeval and M. Sakellariadou, JCAP 1010, 003 (2010) doi:10.1088/1475-7516/2010/10/003 [arXiv:1006.0931 [astro-ph.CO]].

28. J. J. Blanco-Pillado, K. D. Olum and B. Shlaer, Phys. Rev. D 92, no. 6, 063528 (2015) doi:10.1103/PhysRevD.92.063528 [arXiv:1508.02693 [astro-ph.CO]].

29. M. Hindmarsh, J. Lizarraga, J. Urrestilla, D. Daverio and M. Kun arXiv :1703.06696 [astro-ph.CO].

30. J. Canny, A computational approach to edge detection, IEEE Trans. Pattern Analysis and Machine Intelligence 8, 679 (1986).

31. S. Amsel, J. Berger and R. H. Brandenberger, Detecting Cosmic Strings in the CMB with the Canny Algorithm, JCAP 0804, 015 (2008) doi:10.1088/1475-7516/2008/04/015 [arXiv:0709.0982 [astro-ph]].

32. A. Stewart and R. Brandenberger, Edge Detection, Cosmic Strings and the South Pole Telescope, JCAP 0902, 009 (2009) doi:10.1088/1475-7516/2009/02/009 [arXiv:0809.0865 [astro-ph]].

33. R. J. Danos and R. H. Brandenberger, Canny Algorithm, Cosmic Strings and the Cosmic Microwave Background, Int. J. Mod. Phys. D 19, 183 (2010) doi:10.1142/S0218271810016324 [arXiv:0811.2004 [astro-ph]].

34. L. Hergt, A. Amara, R. Brandenberger, T. Kacprzak and A. Refregier, Searching for Cosmic Strings in CMB Anisotropy Maps using Wavelets and Curvelets, arXiv:1608.00004 [astro-ph.CO].

35. L. Perivolaropoulos, COBE versus cosmic strings: An Analytical model, Phys. Lett. B 298, 305 (1993) [hep-ph/9208247].
36. R. Ciuca, O. F. Hernandez and M. Wolman, A Convolutional Neural Network For Cosmic String Detection in CMB Temperature Maps, arXiv:1708.08878 [astro-ph.CO].
37. J. D. McEwen, S. M. Feeney, H. V. Peiris, Y. Wiaux, C. Ringeval and F. R. Bouchet, Wavelet-Bayesian inference of cosmic strings embedded in the cosmic microwave background, arXiv:1611.10347 [astro-ph.IM].
38. R. H. Leike and T. A. Enlin, Optimal Belief Approximation, ArXiv e-prints (2016), arXiv:1610.09018 [math.ST].
39. Y. LeCun, Y. Bengio, G. Hinton, "Deep learning", Nature, 521:436-444, May 2015.
40. Edmund J. Copeland, T.W.B. Kibble ;Cosmic Strings and Super strings, 2009
41. J. Copeland, Edmund C. Myers, Robert Polchinski, Joseph. (2004). Cosmic superstrings II. Comptes Rendus Physique - C R PHYS. 5. 1021-1029.
42. Shai Shalev-Shawartz and Shai Ben-David "Understanding Machine Learning", Cambridge University Press.
43. K.P. Murphy "Machine learning :a probabilistic perspective," ,2012,MIT Press,Cambridge,MA.
44. T.Hastie,R.Tibshirani,J.Freidman,"The Elements of Statistical Learning, "2009,Springer,New York.

45. I. Goodfellow, Y. Bengio, A. Courville, "Deep Learning" 2017, MIT Press Cambridge, MA
46. K. Hornik, M. Stinchcombe, H. White, "Multilayer feedforward networks are universal approximators" *Neural Network*, 1989, 2(5), pp. 359-366.
47. L. Perivolaropoulos, COBE versus cosmic strings: An Analytical model, *Phys. Lett. B* 298, 305 (1993) [hep-ph/9208247].
48. E. Howell (2016, August 19). Cosmic Microwave Background: Remnant of the Big Bang. Retrieved from <https://www.space.com/33892-cosmic-microwave-background.html>
49. V. Dumoulin, F. Visin, "A guide to convolution arithmetic for deep learning", arXiv e-prints (2016), arXiv:1603.07285 [stat.ML]
50. A. A. Fraisse, C. Ringeval, D. N. Spergel and F. R. Bouchet, Small-Angle CMB Temperature Anisotropies Induced by Cosmic Strings, *Phys. Rev. D* 78, 043535 (2008) doi:10.1103/PhysRevD.78.043535 [arXiv:0708.1162 [astro-ph]].
51. K. He, X. Zhang, S. Ren, J. Sun, Deep Residual Learning for Image Recognition. *CVPR* 2016: 770-778, [arXiv:1512.03385]
53. R. Ciuca and O. F. Hernandez, A Bayesian Framework for Cosmic String Searches in CMB Maps, *JCAP* 1708, no. 08, 028 (2017) doi:10.1088/1475-7516/2017/08/028 [arXiv:1706.04131 [astro-ph.CO]].
54. T. Lin, P. Goyal, R. Girshick, K. He, P. Dollr "Focal Loss for Dense Object Detection", arXiv e-prints (2018), arXiv:1708.02002v2

55. Copeland, Edmund J; Myers, Robert C; Polchinski, Joseph (2004). "Cosmic F- and D-strings". *Journal of High Energy Physics*. 2004 (6): 013. arXiv:hep-th/0312067. Bibcode:2004JHEP...06..013C. doi:10.1088/1126-6708/2004/06/013.

56. Aspinwall, Paul; Bridgeland, Tom; Craw, Alastair; Douglas, Michael; Gross, Mark; Kapustin, Anton; Moore, Gregory; Segal, Graeme; Szendri, Balzs; Wilson, P.M.H., eds. (2009). *Dirichlet Branes and Mirror Symmetry*. Clay Mathematics Monographs . 4. American Mathematical Society. ISBN 978-0-8218-3848-8.

57. P. van Nieuwenhuizen, *Phys. Rep.* 68, 189 (1981)

58. Wikipedia contributors. (2018, July 27). Cosmic string. In Wikipedia, The Free Encyclopedia. Retrieved 16:57, August 6, 2018, from https://en.wikipedia.org/w/index.php?title=Cosmic_string&oldid=852180294